

Optimal self-assembly of Rydberg excitations for quantum gate operations

Martin Gärtner,^{1,2,3} Kilian P. Heeg,¹ Thomas Gasenzer,^{2,3} and Jörg Evers¹

¹*Max-Planck-Institut für Kernphysik, Saupfercheckweg 1, 69117 Heidelberg, Germany*

²*Institut für Theoretische Physik, Ruprecht-Karls-Universität Heidelberg, Philosophenweg 16, 69120 Heidelberg, Germany*

³*ExtreMe Matter Institute EMMI, GSI Helmholtzzentrum für Schwerionenforschung GmbH, Planckstraße 1, 64291 Darmstadt, Germany*

(Dated: October 15, 2019)

We study off resonantly driven disordered gases of Rydberg atoms showing that strong correlation and non-trivial spatial ordering of excitations arise. As an application an implementation of the three-atom CSWAP or Fredkin gate with Rydberg atoms is discussed. The gate not only exploits the Rydberg blockade, but also utilizes the special features of an asymmetric geometric arrangement of the three atoms. We show that continuous-wave off-resonant laser driving alone is sufficient to create Rydberg excitations in the required spatial arrangement out of a homogeneous cloud of atoms, thus optimizing the gate fidelity automatically.

PACS numbers: 67.85.-d, 32.80.Ee, 42.50.Nn

Highly excited Rydberg atoms have extreme properties which make them promising candidates for a number of fascinating applications [1, 2]. Most importantly, they feature long-range van der Waals (vdW) interactions, which lead to a dipole blockade [3, 4]. After initial work on bulk properties of Rydberg ensembles, current effort focuses more and more on spatially resolved observations, fueled by experimental progress [5, 6] and theoretical proposals [7, 8] for spatially resolved excitation imaging. Also on the theoretical side, in particular rate equation models [9, 10] and full many-body simulations on truncated Hilbert spaces [11–15] provide a handle to access spatially resolved properties.

In this spirit, it has been predicted that spatial pair correlations can be induced in a three-level Rydberg gas via the so-called anti-blockade arising from resonant excitations due to single-atom Autler-Townes splitting [16]. These correlations could be measured based on mechanical forces due to the vdW interaction. The induced particle motion leads to an encoding of position correlations into a time-dependent Penning ionization signal [17]. Interestingly, in this way, spatial information is gained without a spatially resolved measurement. Following these works on spatial properties of pairs of Rydberg atoms in large ensembles, it was subsequently shown that also the Rydberg ensemble as a whole could form crystalline structures in the Rydberg excitation density [18–20]. It was proposed that such ground-state crystals (GSC) could be produced using chirped laser pulses [18, 19]. The chirp of the laser driving induces adiabatic passage to the energetically most favorable state corresponding to the crystalline excitation structure. Recently, it has been shown that spatial correlations also arise for resonantly driven atoms [6], which can be understood from entropic arguments [21].

However, so far, only few applications of regular excitation structures have been suggested, such as the study of exotic phases of spin lattices [22, 23], a quantum bus

based on GSC [24], and the creation of correlated photon states [25].

Here, we study regular excitation structures that arise in an off-resonantly driven gas, and show that their unique properties can be used to construct a quantum gate. In particular, well-defined structures of multiple excitations with two different inter-atomic distances can be created. We show how such a structure can be exploited to implement a controlled-swap quantum gate, in which one atom acts as a control for the dynamics of two other atoms. We find that the gate fidelity sensitively depends on the specific geometric arrangement of the excited atoms. High fidelity is achieved, as our resonant excitation scheme automatically self-assembles the optimum arrangement out of a homogeneous cloud of atoms, independent of the laser parameters. The two characteristic inter-atomic distances differ by a universal factor of $2^{1/d}$ for an interaction potential $V \sim 1/r^d$, also independent of the laser parameters. We show that the desired excitation structure arises dynamically for off-resonant laser excitation, without the need for laser chirping, and can extend over the entire cloud. Unlike previously studied GSC, its properties are determined by the interaction between the atoms, and are independent of the trap size. Consequently, all relevant observables characterizing the excitation structure yield results qualitatively different from those for the GSC.

Our model system is a one-dimensional cloud of Rydberg atoms in two-level and frozen-gas approximations [2]. We assume temporally and spatially constant laser intensity and wavelength. The corresponding many-body Hamiltonian in a suitable interaction picture and rotating wave approximation reads ($\hbar = 1$) [2, 11, 12]

$$H = \sum_{i=1}^N \left[-\Delta s_{ee}^{(i)} + \frac{\Omega}{2} \sigma_x^{(i)} \right] + C_6 \sum_{i < j}^N \frac{s_{ee}^{(i)} s_{ee}^{(j)}}{r_{ij}^6}, \quad (1)$$

with $s_{\alpha\beta}^{(i)} = |\alpha\rangle_i \langle\beta|$ and $\sigma_x^{(i)} = s_{eg}^{(i)} + s_{ge}^{(i)}$ for atom i .

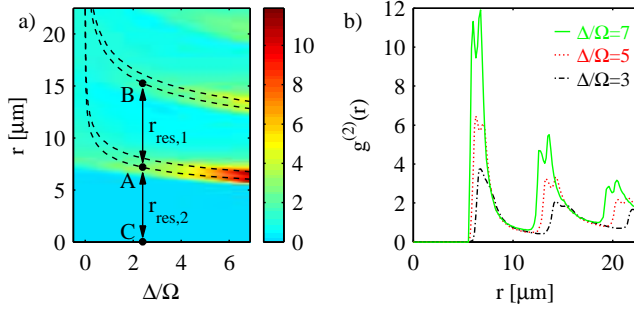


FIG. 1. (Color online) (a) Pair correlation function $g^{(2)}(r)$ as a function of interparticle distance r and detuning Δ . Dashed lines are theoretical predictions for resonances explained in the text. (b) Sections through (a) at detunings $\Delta/\Omega = 3, 5, 7$. Parameters are $L = 30 \mu\text{m}$, $N = 30$, $\Omega = 10 \text{ MHz}$, and $C_6 = 660 \text{ GHz } \mu\text{m}^6$.

The first part of H is a sum over single-atom contributions. It includes the detuning Δ between laser frequency and atomic transition frequency, and the laser coupling between the ground state $|g\rangle$ and Rydberg state $|e\rangle$ with Rabi frequency Ω . The second part accounts for the vdW interactions between two atoms in the Rydberg state at a mutual distance r_{ij} . We numerically solve the time dependent Schrödinger equation with Hamiltonian (1) for given atom positions \mathbf{r}_i and parameters C_6 , Ω , and Δ , starting from an initial state with all atoms in the ground state, on a suitably truncated Hilbert space, assisted by Monte Carlo sampling over different realizations of the geometrical arrangement of the atoms [12, 26–28]. We use generic parameters $\Omega = 10 \text{ MHz}$ and $C_6 = 660 \text{ GHz } \mu\text{m}^6$, which however can be mapped to any other parameter values by rescaling time and length. For these parameters, the systems studied here typically converge at physical evolution times of about $2 \mu\text{s}$, while the reported observables have been obtained at time $5 \mu\text{s}$.

As a first step, we show that our approach enables us to generate characteristic geometric excitation structures out of the homogeneous cloud of atoms, which will form the basis for the implementation of the quantum gate in the second part. For this we study the pair correlation function $g^{(2)}(r) = N_p(r)^{-1} \sum'_{i,j} \langle s_{ee}^i s_{ee}^j \rangle / (\langle s_{ee}^i \rangle \langle s_{ee}^j \rangle)$, where $\sum'_{i,j}$ sums over pairs with distance in $[r, r + \Delta r]$ and $N_p(r)$ is the total number of such pairs. $g^{(2)}(r)$ is a measure for the conditioned probability for an excitation if another excitation is already present at a distance r . As shown in Fig. 1, pronounced resonances emerge in $g^{(2)}$ at regularly spaced distances for detunings $\Delta > \Omega$. At large detunings ($\Delta/\Omega \gg 1$) and without the interaction ($C_6 \rightarrow 0$), the laser field is off-resonant with all transitions and does not induce excitations. But if the vdW interaction is included, it can shift transitions to higher excited states into resonance with the laser [16, 17, 29]. A closer look at Fig. 1 reveals a sequence of double res-

onances. The first resonance at lowest interparticle distance is the well-known resonant pair excitation [16] in which the ground state is resonantly coupled to a doubly excited state via two-photon excitation if $2\Delta = C_6/r_{\text{res},2}^6$. We identified the second maximum at slightly higher r as the resonant transition from an m -fold to an $m+1$ -fold excited state, satisfying $\Delta = C_6/r_{\text{res},1}^6$. The two conditions are shown as dashed lines in Fig. 1(a) and coincide very well with the maxima of $g^{(2)}$ from the numerical simulation results. Starting from a doubly-excited state with inter-atomic distance $r_{\text{res},2}$, a triply excited state emerges. For the later analysis it is crucial to note that the third atom has distance $r_{\text{res},1} \neq r_{\text{res},2}$, such that an asymmetric three-particle structure is created. This triplet causes the third resonance line at $r_{\text{res},1} + r_{\text{res},2}$ in Fig. 1(a). Subsequent resonances originate from higher-excited states, which most likely occur again at distances $r_{\text{res},1}$ from the respective previous structures. In total, for highly excited states, a regular chain of atoms with a single “defect” formed by the initial pair of atoms is created due to the structure of the interaction potential.

Interestingly, the triply excited state is distinguished by a universal ratio $r_{\text{res},1}/r_{\text{res},2} = 2^{1/d}$ for an interaction potential $V \sim 1/r^d$, independent of the trap size and the laser parameters. In this sense, the interaction potential leads to a robust self-assembly of asymmetric excitation structures. This invites applications exploiting the robust and definite asymmetric spatial configuration with distances $r_{\text{res},1}$ and $r_{\text{res},2}$ between the excitations, created out of a homogeneous cloud of atoms.

In the second step, we now turn to a specific application exploiting the spatially asymmetric excitation structure, and show that the generated spatial structures indeed are optimal. For this we consider an implementation of a three-particle quantum gate [1, 30–32]. Based on the approach used in Ref. [6], the excitation structure generated in the first step can be isolated by removing ground state atoms with a resonant laser pulse, and subsequently mapped onto ground states by resonantly driving a transition to a rapidly decaying p -state. That way, a spatial arrangement of ground state atoms is prepared, that corresponds to one specific realization of the original excitation structure. In the case that three atoms survive this procedure, their mutual distances are $r_{\text{res},2}$, $r_{\text{res},1}$, and $r_{\text{res},2} + r_{\text{res},1}$, and we denote the three atoms as C , A and B as indicated in Fig. 1(a), respectively.

We exploit this asymmetric arrangement of atoms to implement a controlled SWAP (CSWAP) or Fredkin gate. Depending on the state of the control atom C , atoms A and B shall interchange their states or not. The qubits are stored in two hyperfine components of the ground state $|0\rangle$ and $|1\rangle$ that can both be coupled to the Rydberg state $|e\rangle$. The gate protocol consisting of five laser pulses is illustrated in Fig. 2(a). As an example, two possible evolution sequences for initial states $|CAB\rangle = |010\rangle$ or $|110\rangle$ out of the full truth table are shown in the bot-

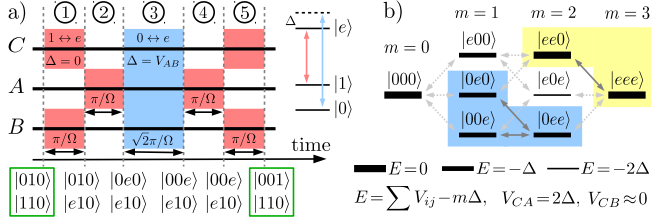


FIG. 2. (Color online) (a) Illustration of the gate protocol and level scheme of a single atom. The truth table is given for two exemplary initial states $|CAB\rangle = |010\rangle$ and $|110\rangle$. Depending on the control bit C bits A and B interchange their states, or not. (b) Hamiltonian of the detuned pulse (blue in gate protocol). The thickness of the bars stands for the value E of the diagonal element of the corresponding state (with m Rydberg excitations). Double arrows indicate laser couplings. In the blue subspace, the state $|0e0\rangle$ evolves into $|00e\rangle$ under the $\sqrt{2}\pi$ -pulse.

tom part of Fig. 2(a). In step 1, a resonant π -pulse on atoms C and B evolves them to $|e\rangle$ if they are initially in $|1\rangle$, but leaves them untouched if they are in $|0\rangle$. Step 2 is a resonant π -pulse on atom A . Again, it induces excitations of A from $|1\rangle$, but not from $|0\rangle$. But due to the excitation blockade, in addition the excitation only occurs if neither C nor B are excited. Therefore, atom A is excited in this step for initial state $|010\rangle$, but not for initial state $|110\rangle$, see Fig. 2(a). The crucial step is the detuned $\sqrt{2}\pi$ -pulse (step 3) in the middle of the sequence applied to all three atoms. The corresponding effective Hamiltonian is shown schematically in Fig. 2(b). Because of the detuning, it decomposes into several approximately independent subspaces. Due to this separation, its main effect is an interchange of states $|0e0\rangle$ and $|00e\rangle$. Besides this desired exchange, also $|ee0\rangle$ would be resonantly coupled to $|eee\rangle$ causing unwanted dynamics. But due to the blockade in the second step, $|ee0\rangle$ and $|eee\rangle$ are never accessed, such that this channel can be neglected. Steps 4 and 5 repeat the first two steps in reverse order, and effectively evolve the atoms back into a superposition of ground states $|0\rangle$ and $|1\rangle$.

We have implemented this five-step sequence on the full three-atom state space and numerically simulated the dynamics. To quantify the quality of the gate for arbitrary input states, we use the gate fidelity $F_{\text{gate}} = \sum_i |\langle \Psi^{(i)} | \Psi_{\text{id}}^{(i)} \rangle|^2 / 8$, where $\Psi_{\text{id}}^{(i)}$ and $\Psi^{(i)}$ are the ideal target and the numerically obtained output state, respectively, as well as the confidence F_{bell} with which a maximally entangled state $|\Psi\rangle_{\text{bell}} = (|001\rangle - |110\rangle) / \sqrt{2}$ can be prepared from the unentangled initial state $(|010\rangle + |110\rangle) / \sqrt{2}$. Figure 3(a) shows F_{gate} as a function of Δ/Ω and the deviation δr of r_{AB} from $r_{\text{res},1}$. The fidelity increases with Δ/Ω since the decomposition of the Hamiltonian into independent subspaces improves with Δ . We also find that F_{gate} is very sensitive to variations in r_{AB} , and reaches the optimum value only for $\delta r = 0$. In

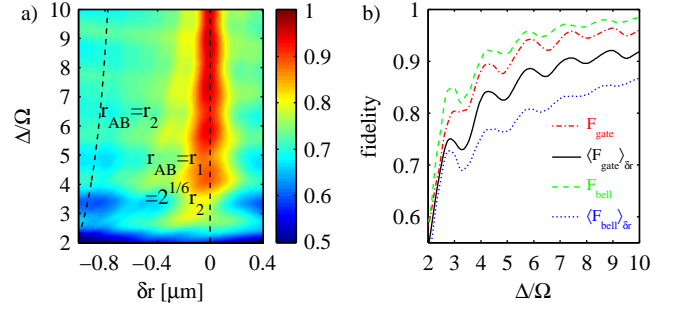


FIG. 3. (Color online) (a) Fidelity F_{gate} of the CSWAP gate against detuning Δ and imperfections δr of the spatial arrangement of the three atoms. (b) F_{gate} and F_{bell} for the optimal r_{AB} and averaged over a Lorentzian distribution of distances r_{AB} . The fidelity is relatively insensitive to variations in r_{CA} .

Fig. 3(b) results for both, F_{gate} and F_{bell} , with optimized r_{AB} and integrated over the distribution of distances r_{AB} that results from the preparation using the resonant excitation scheme are shown. We notice that the entanglement fidelity is even more sensitive to variations in r_{AB} than the gate fidelity. The reason is that the Bell state preparation strongly depends on the relative phases that the different product states acquire during the gate operation. These phases are more difficult to control, the higher Δ/Ω becomes. Thus they counteract the decreasing coupling between the subspaces of the Hamiltonian and decrease the fidelity.

It is crucial to realize that the required separation of the Hamiltonian into different subspaces only arises due to the asymmetric distances $r_{CA}/r_{AB} \neq 1$. Furthermore, already small deviations in the optimum distance δr lead to a significant degradation of the gate fidelity. In our setup this optimum distance is automatically achieved for each given laser detuning, because the resonantly excited correlated structures are created with atomic distances such that the laser detuning condition required for the gate operation is satisfied. It is in this sense, that the self-assembly of the excitation structures is optimal.

Experimentally, laser-excited Rydberg atoms in a quasi one-dimensional dipole trap could be used to verify our theoretical predictions. Depending on the capabilities of the experimental setup, different predictions can be probed. Independent of the gate protocol, already the resonant excitation structures can be studied, which have qualitatively different properties compared to those of previously studied GSC.

A first difference arises in the detuning dependence of the total number of Rydberg atoms N_{ryd} , as well in the excitation statistics, which require only a counting the total number of excitations. The excitation statistics is characterized by the Mandel Q parameter $Q = (\langle \hat{N}_{\text{ryd}}^2 \rangle - \langle \hat{N}_{\text{ryd}} \rangle^2) / \langle \hat{N}_{\text{ryd}} \rangle - 1$. For a Poissonian distribution of excitation numbers, like in a coherent state,

the Q parameter is zero, while for sub-Poissonian statistics it is negative. In a GSC, for a given detuning, a definite number of excitations is reached. Then, ideally, Q reaches the value -1 for a Fock state, realized by the unique ground state. In contrast, Fig. 4(a) shows that in our setup, the Q parameter assumes a minimum at some positive detuning, but then increases again towards larger Δ . This is due to the fact that with increasing detuning, the spatial excitation resonances become narrower. As shown in Fig. 4(b), the interaction potential $V(r)$ translates the width of the excitation resonances in energy space into a distance dependence. For the same energy-resonance width, the position-space resonances become narrower as the distance decreases at which the laser moves into resonance. Hence, an increase of the detuning leads to a reduction of the resonant width. Consequently, the total number of excited atoms decreases with increasing Δ since the distance range over which resonant pair excitation is possible shrinks. The probability to reside in the initial state $|g, g, \dots, g\rangle$ thus becomes non-zero at large detunings which leads to a bimodal distribution of excitation number and therefore to increasing values of Q . This interpretation is supported by corresponding results for Q^* evaluated without the ground state fraction, which remains low even for higher detunings Δ . For higher densities, this effect is expected to set in at higher detunings, which is confirmed by the fact that the maximum of N_{ryd} shifts to the right as the atomic density is increased, see Fig. 4(a).

The second difference arises in the spatial excitation density, which can be accessed via position-resolved measurements of the Rydberg excitations [6–8]. While the second-order correlation function (Fig. 1) clearly exhibits a regular structure of possible distances between the excitations, this does not translate into a peaked structure in the spatially resolved excitation density, as it is the case for GSC. Rather, Fig. 4(c) shows that at high detuning, the excitation density has a step-like dependence on the position. This difference can be understood from the fact that resonantly generated excitation structures are not fixed relative to the trap. For example, already in the case of resonant pair excitation the doubly excited states are only populated if the distance between the excited atoms is $r_{\text{res},2}$. Averaging over all possible ways to place such a pair with fixed distance inside the trap, atoms located within one resonant radius from the ends of the trap are excited only half as often as atoms at the center. This explains the outermost edges in the excitation density. The dashed line in Fig. 4(c) indicates the position $r_{\text{res},2}$ away from one edge of the string coinciding with the position of the step in excitation density, clearly supporting this interpretation. The states with three excitations cause the second fringe from the trap end to appear at $r_{\text{res},2} + r_{\text{res},1}$. In higher dimensions the condition of resonant excitation is fulfilled for various positions of the third excitation and thus it is less localized.

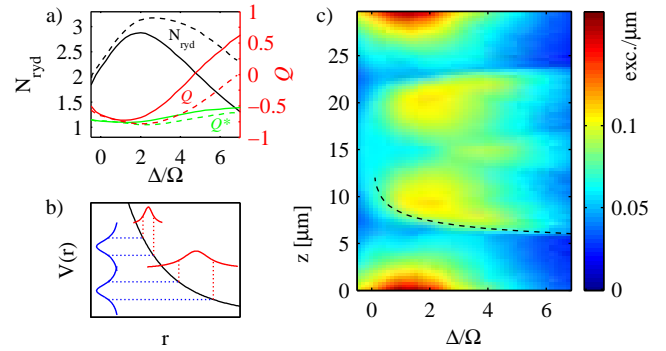


FIG. 4. (Color online) (a) Total number of excited atoms and Mandel Q parameter as a function of the detuning. Q^* is the corresponding parameter evaluated without the ground state fraction. Solid lines show $N = 30$; dashed lines show $N = 45$. C_6 and L are as in Fig. 1. (b) Detuning-dependent transformation of energetic resonances into spatial resonances via the interaction potential $V(r) = C_6/r^6$. Note that, if the slope of the potential curve changes significantly over the width of the resonance, the spatial shape becomes distorted. (c) Rydberg excitation density in excitations per μm vs. position on the string and detuning. Dashed line: resonance line corresponding to $2\Delta = C_6/r^6$ as explained in the text.

Note that in reverse, the resonances in $g^{(2)}$ could be used to determine the precise structure of the interaction potential.

As a third step, the Fredkin gate protocol could be tested experimentally by generating an asymmetric arrangement of three atoms as outlined above, preparing in one of the initial states by single qubit Rabi pulses, applying the gate protocol, and finally determining the success probability, e.g., by state selective fluorescence imaging of the atoms.

In summary, we have shown that strongly correlated excitation structures form at off-resonant laser driving. These structures can extend over the entire trap volume and show two different characteristic lengths having a universal ratio. The such generated structures can be used to implement an efficient three-qubit quantum gate, because the excitation scheme automatically generates an asymmetric spatial arrangement out of a homogeneous atom cloud such that an optimum gate operation is achieved for the given laser parameters. Extensions to other gates like CNOT or Toffoli are straight forward. Resonantly created structures differ from previously studied (ground state) crystals as their spatial arrangement is determined by the laser parameters and the interaction strength rather than by the trap geometry.

This work was supported by University of Heidelberg (Center for Quantum Dynamics, LGFG), by Deutsche Forschungsgemeinschaft (GA 677/7,8), and by the Helmholtz Association (HA216/EMMI).

-
- [1] M. Saffman, T. G. Walker, and K. Mølmer, *Rev. Mod. Phys.* **82**, 2313 (2010).
- [2] D. Comparat and P. Pillet, *J. Opt. Soc. Am. B* **27**, A208 (2010).
- [3] M. D. Lukin, M. Fleischhauer, R. Côté, L. M. Duan, D. Jaksch, J. I. Cirac, and P. Zoller, *Phys. Rev. Lett.* **87**, 037901 (2001).
- [4] D. Jaksch, J. I. Cirac, P. Zoller, S. L. Rolston, R. Côté, and M. D. Lukin, *Phys. Rev. Lett.* **85**, 2208 (2000).
- [5] A. Schwarzkopf, R. E. Sapiro, and G. Raithel, *Phys. Rev. Lett.* **107**, 103001 (2011).
- [6] P. Schauß, M. Cheneau, M. Endres, T. Fukuhara, S. Hild, A. Omran, T. Pohl, C. Gross, S. Kuhr, and I. Bloch, *Nature* **491**, 87 (2012).
- [7] B. Olmos, W. Li, S. Hofferberth, and I. Lesanovsky, *Phys. Rev. A* **84**, 041607 (2011).
- [8] G. Günter, M. Robert-de Saint-Vincent, H. Schempp, C. S. Hofmann, S. Whitlock, and M. Weidemüller, *Phys. Rev. Lett.* **108**, 013002 (2012).
- [9] C. Ates, T. Pohl, T. Pattard, and J. M. Rost, *Phys. Rev. A* **76**, 013413 (2007).
- [10] K. P. Heeg, M. Gärttner, and J. Evers, *Phys. Rev. A* **86**, 063421 (2012).
- [11] F. Robicheaux and J. V. Hernández, *Phys. Rev. A* **72**, 063403 (2005).
- [12] K. C. Younge, A. Reinhard, T. Pohl, P. R. Berman, and G. Raithel, *Phys. Rev. A* **79**, 043420 (2009).
- [13] H. Weimer, R. Löw, T. Pfau, and H. P. Büchler, *Phys. Rev. Lett.* **101**, 250601 (2008).
- [14] B. Olmos, R. González-Férez, and I. Lesanovsky, *Phys. Rev. A* **79**, 043419 (2009).
- [15] N. Tezak, M. Mayle, and P. Schmelcher, *J. Phys. B* **44**, 184009 (2011).
- [16] C. Ates, T. Pohl, T. Pattard, and J. M. Rost, *Phys. Rev. Lett.* **98**, 023002 (2007).
- [17] T. Amthor, C. Giese, C. S. Hofmann, and M. Weidemüller, *Phys. Rev. Lett.* **104**, 013001 (2010).
- [18] T. Pohl, E. Demler, and M. D. Lukin, *Phys. Rev. Lett.* **104**, 043002 (2010).
- [19] R. M. W. van Bijnen, S. Smit, K. A. H. van Leeuwen, E. J. D. Vredenbregt, and S. J. J. M. F. Kokkelmans, *J. Phys. B* **44**, 184008 (2011).
- [20] J. Schachenmayer, I. Lesanovsky, A. Micheli, and A. J. Daley, *New Journal of Physics* **491**, 103044 (2010).
- [21] C. Ates and I. Lesanovsky, *Phys. Rev. A* **86**, 013408 (2012).
- [22] H. Weimer and H. P. Büchler, *Phys. Rev. Lett.* **105**, 230403 (2010).
- [23] E. Sela, M. Punk, and M. Garst, *Phys. Rev. B* **84**, 085434 (2011).
- [24] H. Weimer, N. Y. Yao, C. R. Laumann, and M. D. Lukin, *Phys. Rev. Lett.* **108**, 100501 (2012).
- [25] B. Olmos and I. Lesanovsky, *Phys. Rev. A* **82**, 063404 (2010).
- [26] M. Gärttner, K. P. Heeg, T. Gasenzer, and J. Evers, *Phys. Rev. A* **86**, 033422 (2012).
- [27] T. J. Carroll, C. Daniel, L. Hoover, T. Sidie, and M. W. Noel, *Phys. Rev. A* **80**, 052712 (2009).
- [28] I. I. Ryabtsev, D. B. Tretyakov, I. I. Beterov, V. M. Entin, and E. A. Yakshina, *Phys. Rev. A* **82**, 053409 (2010).
- [29] M. Mayle, W. Zeller, N. Tezak, and P. Schmelcher, *Phys. Rev. A* **84**, 010701 (2011).
- [30] M. Saffman and T. G. Walker, *Phys. Rev. A* **72**, 022347 (2005).
- [31] I. E. Protsenko, G. Reymond, N. Schlosser, and P. Grangier, *Phys. Rev. A* **65**, 052301 (2002).
- [32] L. Isenhower, E. Urban, X. L. Zhang, A. T. Gill, T. Henage, T. A. Johnson, T. G. Walker, and M. Saffman, *Phys. Rev. Lett.* **104**, 010503 (2010).